





Synthesis of Power Line Notch Filter in Wearable Biomedical Devices for Wireless Body Area Network

Aruna Pathak¹, Chandan Kumar Choubey^{2*}

¹ Department of Electronics and Communication, Government Engineering College, Bharatpur, Rajasthan 321001, India

² Symbiosis Institute of Technology, Symbiosis International (Deemed University), Pune Campus, Maharashtra 412115, India

Corresponding Author Email: guru.chandan@gmail.com

<https://doi.org/10.18280/mmp.100537>

ABSTRACT

Received: 9 June 2023

Revised: 20 August 2023

Accepted: 4 September 2023

Available online: 27 October 2023

Keywords:

notch filter, wireless body area network, power-line interference, voltage differencing gain amplifier

With the rising prevalence of wearable biomedical devices for recording diverse biosignals, the potential for inaccurate interpretations due to noise susceptibility, including false alarms and misdiagnoses, is increasingly recognized. This study presents the systematic design and evaluation of a current-mode-based active notch filter aimed at eliminating the pervasive power-line interference (PLI) that corrupts biosignals. The filter is constructed using a modern and versatile current-mode analog building block (ABB), specifically the voltage differencing gain amplifier (VDGA). The design of this second-order filter incorporates a single VDGA as an active component and two capacitors as passive components, eliminating the need for resistors. Employing this filter, the influence of the 50Hz PLI on biological signals is effectively suppressed. The filter exhibits desirable properties of the current-mode circuit, including reduced power consumption, an expanded dynamic range, and enhanced accuracy. Key parameters of the filter, such as the pole frequency and the quality factor, can be electronically adjusted and orthogonally tuned via the bias currents of the VDGA. To validate its functionality, the proposed filter design was simulated using the PSPICE simulator with the MAX435 IC's macro-model. The simulation results revealed a notch depth and total harmonic distortion (THD) of -52.9 dB and -55 dB, respectively. The performance of this filter was subsequently compared with existing analog notch filters detailed in the literature. Given its efficacy and simplicity, the proposed filter is deemed suitable for deployment in high-performance biomedical detection equipment.

1. INTRODUCTION

Wearable devices find utility in a diverse range of applications, spanning healthcare, early diagnosis, rehabilitation, monitoring, and wellness. The need for continuous surveillance necessitates the use of wearable technology, which enables individuals to maintain their daily routines, rendering monitoring more effective compared to prolonged stays in healthcare facilities [1]. The interest in wearable devices for healthcare is amplified by aging populations, as these devices foster independence by allowing individuals to reside at home while being adequately monitored.

A wireless body area network (WBAN) facilitates real-time health monitoring without disturbing an individual's daily activities [2]. As depicted in Figure 1, a wearable device gathers health-related data and wirelessly transmits this information to a smart device [3]. The data is stored and processed either on a smart device or in the cloud, and wellness details, alongside the results of the received signals, can be relayed to several end users. In a healthcare application, these users comprise the device wearer, caregivers, medical professionals, and family and friends.

Despite their advantages, wearable devices encounter unique challenges when processing low-frequency biomedical signals, compared to non-wearable devices. These challenges include power-line interference (PLI), motion artifacts, and

contact with body-conforming components. Owing to this susceptibility to noise and artifacts, the signals derived from wearable technology may lead to incorrect interpretations, such as false alarms and medical errors [4–8]. This study aims to evaluate the quality of biosignals to mitigate concerns associated with poor-quality signals, like false alarms. Given that most biosignals possess low amplitudes [9], pre-amplification and filtering are deemed essential prior to further digital signal processing.

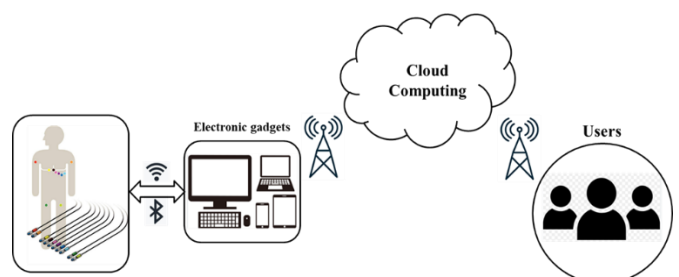


Figure 1. Wearable device and its data path

As illustrated in Figure 2, a standard biosignal processing system encompasses sensors or transducers that transform biosignals into electrical signals. These signals, typically of small amplitude, are collected and amplified by a preamplifier. To eliminate unwanted noise such as power-line interference

(PLI), a notch filter is integrated into the system. The signals are then converted into a digital format by an analog-to-digital converter. The central processing unit (CPU) subsequently processes these digital signals before they are either displayed or wirelessly transmitted [10].

PLI, typically at frequencies of 50Hz or 60Hz, is a prevalent source of noise during biosignal recording, and is detectable in most healthcare settings [11-14]. To ensure the delivery of reliable signals to subsequent stages, the integration of a notch filter to eradicate PLI is deemed essential.

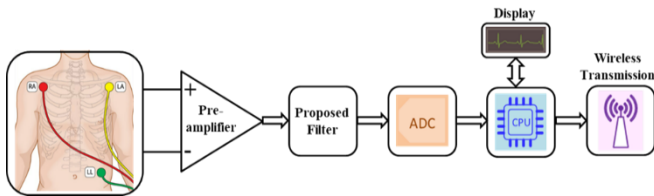


Figure 2. Block diagram of the biosignal detection system

To suppress or attenuate the 50Hz or 60Hz PLI, a variety of analog notch filters designed with distinct active blocks have been proposed by several researchers, aimed at processing different types of biomedical signals. These circuits, which employ current-mode active blocks such as the second-generation current conveyor (CCII) [15-17], differential difference current conveyor (DDCC) [18], and differential voltage current conveyor (DVCC) [19], hold distinct advantages, including a larger dynamic range, simpler circuit architecture, and lower power consumption.

Notch filters based on an op-amp have been proposed to remove power line interference at 60Hz [20] and 50Hz [21]. An OTA-based universal biquad filter utilizing 0.5µm CMOS technology is described in the study [22], and a universal biquad filter based on a DVCC, employing 0.35µm CMOS technology, is proposed in the study [19]. An op-amp-based filter for biopotential acquisition systems to eliminate power line interference is discussed in the study [23]. An OTA-C low-pass notch filter for EEG application, designed with 0.18µm CMOS technology, is introduced in the study [24], and another OTA-based low-pass and notch filter using the same technology is proposed in the study [25]. Biquad filters employing a voltage-differencing differential input buffered amplifier (VD-DIBA) are suggested in the study [26].

Among the most versatile and practical current-mode building blocks available is the voltage differencing gain amplifier (VDGA) [27-30]. In the pursuit of efficiently minimizing or diminishing PLI from low-frequency biosignals, such as ECG, EEG, and EMG signals, this study introduces a novel notch filter utilizing a VDGA. Thus, a VDGA-based notch filter suitable for IC implementation is proposed.

2. CIRCUIT DESCRIPTION

2.1 Voltage differencing gain amplifier

As the proposed notch filter utilizes VDGA as an active element, the VDGA is introduced and discussed in this sub-section. The voltage differencing gain amplifier (VDGA), a versatile current-mode active building block based on the voltage differencing transconductance amplifier (VDTA) [31], was introduced to the analog domain in 2013 [30]. Figure 3 depicts the VDGA's schematic symbol. In Eq. (1), the port

relationship of VDGA is provided in matrix form. A VDGA can be implemented most easily with three OTAs because it needs three transconductance gains [32], as the OTA IC MAX435 is one of the most efficient commercially available ICs. Figure 4 illustrates the OTA-based implementation of the VDGA.

$$\begin{bmatrix} I_P \\ I_N \\ I_Z \\ I_X \\ I_W \\ I_{VW} \end{bmatrix} = \begin{bmatrix} 0 & 0 & 0 & 0 & 0 \\ 0 & 0 & 0 & 0 & 0 \\ g_{mA} & -g_{mA} & 0 & 0 & 0 \\ 0 & 0 & g_{mB} & 0 & 0 \\ 0 & 0 & -g_{mB} & 0 & g_{mC} \\ 0 & 0 & \beta & 0 & 0 \end{bmatrix} \begin{bmatrix} V_P \\ V_N \\ V_Z \\ V_X \\ V_W \end{bmatrix} \quad (1)$$

where, $\beta = \frac{g_{mB}}{g_{mC}}$.

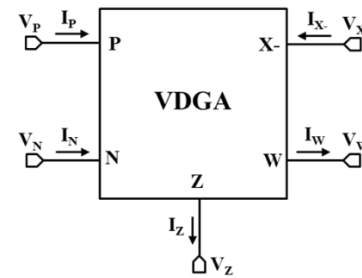


Figure 3. Schematic symbol of the VDGA

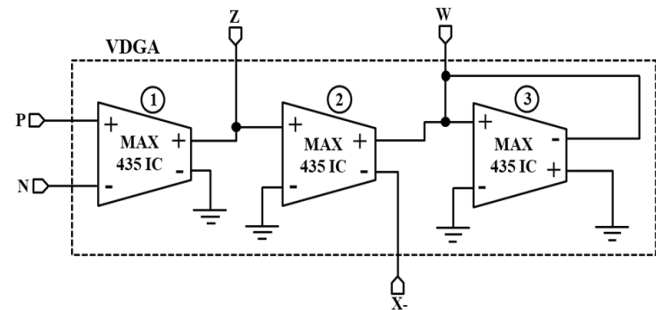


Figure 4. OTA-based implementation of the VDGA

2.2 Realization of power-line notch filter

To remove an unwanted PLI from biosignals, a notch filter is designed and discussed in this sub-section. It is designed by increasing the quality factor of a band-reject filter (BRF) by properly adjusting its passive components. A BRF permits the transmission of frequencies outside of a given frequency band while rejecting or blocking the transmission of frequencies inside that range. When the quality factor of a BRF is increased, the width of the stop band becomes narrower, and hence it behaves like a notch filter by stopping some selective frequencies. The general transfer function of a notch filter is expressed as Eq. (2):

$$H(s) = \frac{s^2 + \omega_0^2}{s^2 + s\frac{\omega_0}{Q} + \omega_0^2} \quad (2)$$

The proposed notch filter is therefore designed based on a novel active element, VDGA, to simplify the integrated circuit implementation. The circuit diagram of the proposed filter using VDGA and two capacitors is shown in Figure 5. By

routine analysis, the transfer function of the proposed filter is obtained as Eq. (3):

$$H(s) = \frac{V_{OUT}}{V_{IN}} = \frac{s^2 + \frac{g_{mA}g_{mB}}{C_1C_2}}{s^2 + \frac{s g_{mC}}{C_2} + \frac{g_{mA}g_{mB}}{C_1C_2}} \quad (3)$$

where, g_{mA} , g_{mB} , and g_{mC} are transconductance gains of the VDGA. On comparing Eq. (3) with Eq. (2), we obtained the pole-frequency (f_0) and quality-factor (Q) as follows:

$$f_0 = \frac{1}{2\pi} \sqrt{\frac{g_{mA}g_{mB}}{C_1C_2}} \quad (4)$$

$$Q = \frac{1}{g_{mC}} \sqrt{\frac{g_{mA}g_{mB}C_2}{C_1}} \quad (5)$$

From Eq. (4) and Eq. (5), it can be observed that the filter's parameters are tunable by adjusting the transconductance gains through the bias currents of the VDGA. Furthermore, and have orthogonal tunability by tuning the for first and then the for Q without affecting the parameter.

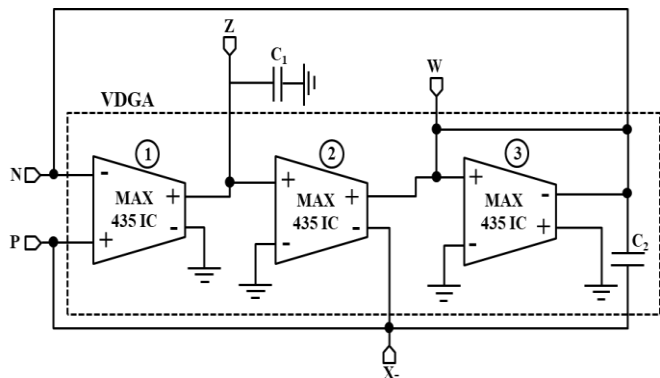


Figure 5. Realization of power line notch filter using VDGA

3. SIMULATION AND RESULTS

To check the functionality of the proposed filter, shown in Figure 5, is simulated in PSPICE software. The macro-model of IC MAX435 is used to realise the VDGA in the simulation. This IC is a highly efficient dual output OTA. It is manufactured by Maxim Integrated. The supply voltages, VDD and VSS, are taken as +9 V and -9 V, respectively.

3.1 Frequency response

The simulated frequency magnitude response of the proposed filter is shown in Figure 6(a). It notches at 50Hz with total attenuation gain of -52.9 dB. Also, the phase response, shown in Figure 6(b), confirms the notching at 50Hz by changing the phase at the said frequency.

3.2 Linearity performance

To check the linearity performance of the proposed filter, total harmonic distortion (THD) is measured for different amplitudes of the input signal in passband at 100Hz frequency.

THD is a measure of unwanted additional signal contents with the input signal. In the passband of the notch filter, THD must be significantly less to pass the signals without any distortion.

It is defined as: $THD = \sqrt{V_2^2 + V_3^2 + \dots + V_n^2} / V_1$, where V_2, V_3, \dots, V_n are the r.m.s value of nth harmonics, and V_1 is the r.m.s value of fundamental components. Figure 7 shows the overall harmonic distortion for a signal at 100Hz, which was used to determine the output quality and dynamic range in the passband. THD is specified as being very low, up to -55 dB. (peak to peak). It signifies that the proposed filter has a large dynamic range.

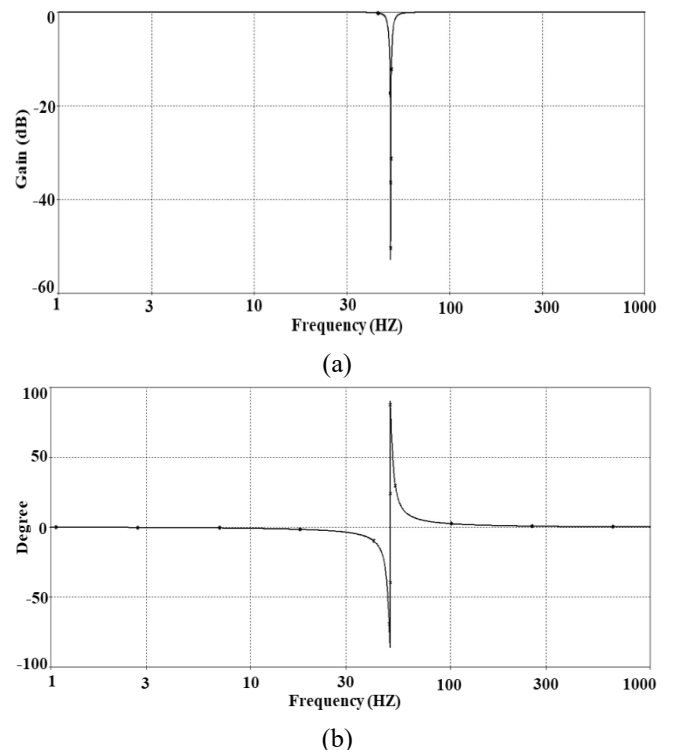


Figure 6. AC analysis response for the proposed notch filter: (a) Magnitude response; (b) Phase response

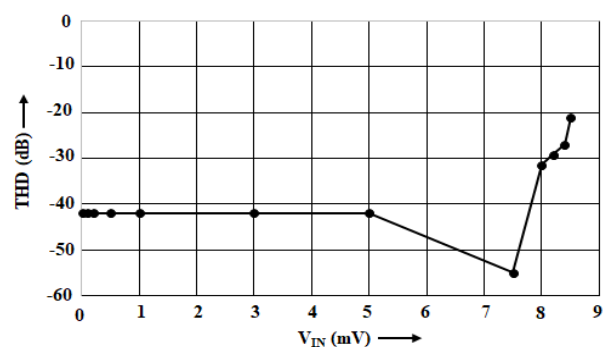


Figure 7. THD of the proposed notch filter

3.3 Biomedical signal testing

To assess the proposed filter's applicability for biomedical applications, it is empirically characterized with a clean ECG signal as input, as illustrated in Figure 8. This ECG signal is generated in PSPICE using the MIT-BIH Arrhythmia database data [33]. Further, the clean ECG signal is contaminated with an artificial PLI of 50Hz generated using sinusoidal

waveforms. Now, The contaminated ECG signal is passed through the proposed notch filter to get the filtered clean ECG signal. The clean ECG, the corrupted ECG, and the filtered ECG signals, along with their FFTs, are shown in Figures 9, 10, and 11, respectively. From Figure 11, it can be observed that the proposed notch filter is effective in suppressing the PLI effectively.

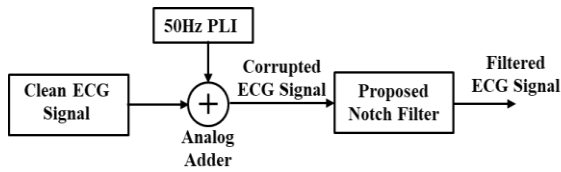


Figure 8. Block diagram of simulation experiment

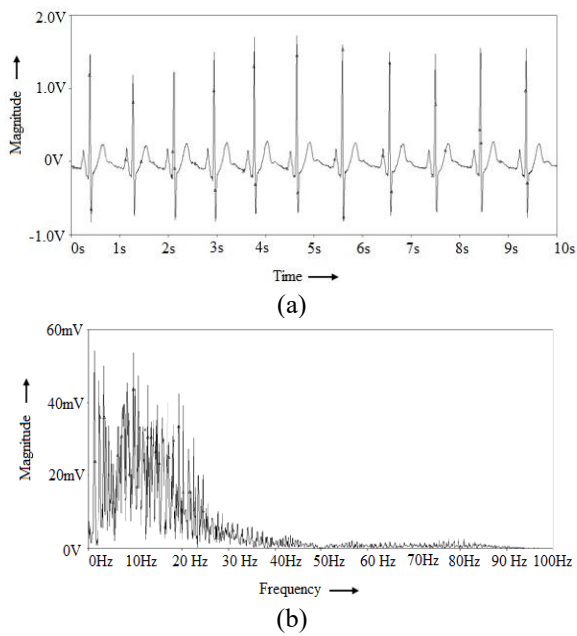


Figure 9. Clean ECG signal in (a) time domain (b) frequency domain

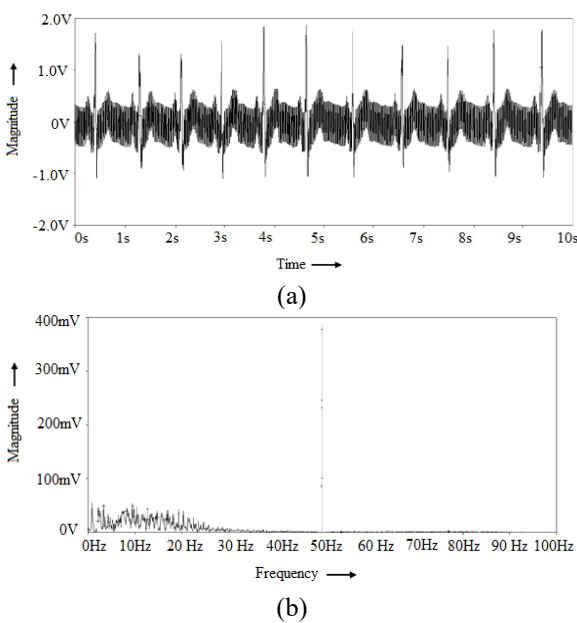


Figure 10. Corrupted ECG signal in (a) time domain; (b) frequency domain

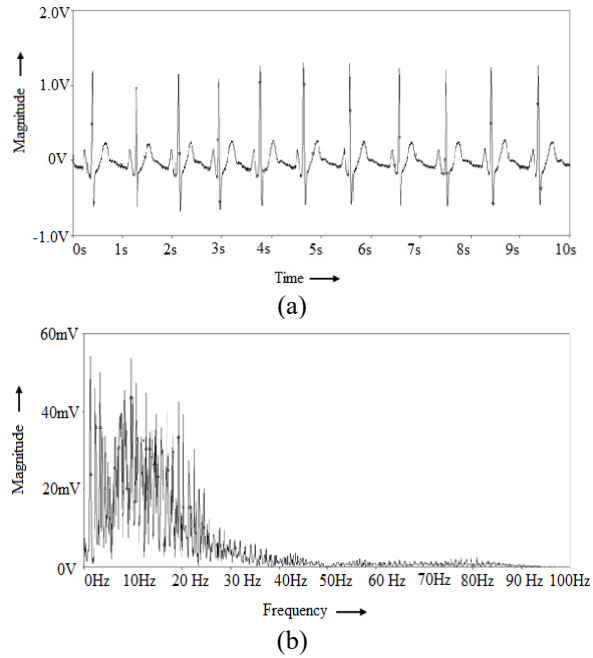


Figure 11. Filtered ECG signal in (a) time domain; (b) frequency domain

4. NON-IDEAL ANALYSIS

The transfer function of the proposed filter given in Eq. (3) and its parameters, f_0 and Q , given in Eq. (4) and Eq. (5), respectively, are derived from the ideal port relationship. In this section, the behavior of a practical filter is analysed by considering the non-ideal port relationship of VDGA as given in Eq. (7).

$$\begin{bmatrix} I_P \\ I_N \\ I_Z \\ I_X \\ I_W \\ I_W \end{bmatrix} = \begin{bmatrix} 0 & 0 & 0 & 0 & 0 \\ 0 & 0 & 0 & 0 & 0 \\ \gamma_A g_{mA} & -\gamma_A g_{mA} & 0 & 0 & 0 \\ 0 & 0 & \gamma_B g_{mB} & 0 & 0 \\ 0 & 0 & -\gamma_B g_{mB} & 0 & \gamma_C g_{mC} \\ 0 & 0 & \frac{\gamma_B}{\gamma_C} \beta & 0 & 0 \end{bmatrix} \begin{bmatrix} V_P \\ V_N \\ V_Z \\ V_X \\ V_W \end{bmatrix} \quad (7)$$

where, $\beta = \frac{g_{mB}}{g_{mC}}$ and γ_A , γ_B and γ_C are transconductance gain errors.

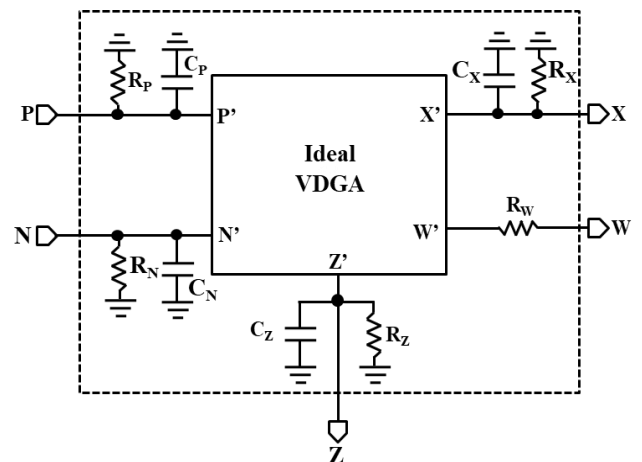


Figure 12. Schematic symbol of the VDGA with parasitics

$$H(s) = \frac{s^2(1 + R_W g_{mc}) + \frac{s(C_Z R_Z + 1)(1 + R_W g_{mc})}{C_1 R_Z} + \frac{g_{mA} g_{mB}}{C_1 C_2}}{s C_1 (1 + R_W g_{mc}) \left[s C_1 + \frac{(s C_Z R_Z + 1)}{R_Z} \right] + g_{mc} \left[s C_1 + \frac{(s C_Z R_Z + 1)}{R_Z} \right] + \left[s C_1 + \frac{(s C_Z R_Z + 1)}{R_Z} \right] \left[\frac{(s C_P R_P + 1)}{R_P} \right] (1 + R_W g_{mc}) + g_{mA} g_{mB}}$$

Table 1. Performance comparison of various implementations of notch filter

| Parameters | Ref. [15] | Ref. [16] | Ref. [17] | Ref. [18] | Ref. [19] | Ref. [20] | Ref. [21] | Ref. [22] | Proposed |
|----------------------------------------|---------------------------|---------------------------|--------------|---------------------------|---------------------------|--------------|---------------------------|---------------------------|--------------|
| VDD | ---- | 1.8V | 2.5V | 2 V | 1.5V | 0.9 | 1.8 V | 0.9 V | 9V |
| Technology | BJT | 0.18µm CMOS | 0.5µm CMOS | 0.35-µm CMOS | 0.18µm CMOS | 0.18µm CMOS | 0.18µm CMOS | 0.18µm CMOS | BJT IC |
| Active blocks | OP-amp-10 | OP-amp-3 | OTA-6, | DVCC-1 | OP-amp-3 | OTA-5 | OTA-3 | VD-DIBA-2 | VDGA-1 |
| Passive element | Resistor-27, Capacitor-03 | Resistor-03, Capacitor-06 | Capacitor-02 | Resistor-02, Capacitor-02 | Resistor-06, Capacitor-03 | Capacitor-04 | Resistor-03, Capacitor-04 | Resistor-02, Capacitor-02 | Capacitor-02 |
| Orthogonal tunability of f_0 and Q | yes | yes | no | no | yes | yes | no | yes | yes |
| Notch frequency | 60Hz | 50Hz | 122.7kHz | 10MHz | 40Hz | 50Hz | 50Hz | 95.50KHz | 50Hz |
| Notch depth | -60dB | -55dB | ---- | ---- | -43dB | -68 dB | ---- | ---- | -52.9 dB |
| THD | ---- | ---- | ---- | ---- | -70dB | -74 dB | -76 dB | 38.75 dB | -55 dB |

Using Eq. (7), the filter's parameters can be obtained by routine analysis as:

$$f_0 = \frac{1}{2\pi} \sqrt{\frac{\gamma_{An} \gamma_{Bn} g_{mA} g_{mBn}}{C_n C_{n-1}}} \quad (8)$$

$$Q = \frac{1}{\gamma_{Cn} g_{mc}} \sqrt{\frac{C_n C_{n-1}}{\gamma_{An} \gamma_{Bn} g_{mA} g_{mB}}} \quad (9)$$

From Eq. (8) and Eq. (9), it can be observed that the filter's parameters, f_0 and Q , are affected by the transconductance gain errors. However, these effects can be tolerated because the values of these gain errors are observed as close to unity for the MAX435 IC in the simulation. The second cause of non-ideality is the presence of parasitics at the various ports of the VDGA, as shown in Figure 12. Now, the transfer function of the proposed filter has been modified as given in Eq. (9).

The values of parasitic capacitances, C_P , C_N , C_Z , and C_X , are found to be very low in the range of a few femto-farads, while the values of parasitic resistances, except R_W , are found to be very high in the range of hundreds of mega-ohms for the MAX435 IC-based VDGA in the simulation. The value of R_W is very low, typically in the range of a few ohms. For these values of parasitics, Eq. (9) can be approximated as the transfer function given in Eq. (3) for the low-frequency operation. The above discussion concludes that the proposed filter is suitable for low-frequency biomedical signals.

5. COMPARISON

The performance of the proposed filter is compared with the available circuits in the literature in terms of the voltage supply, technologies used, active and passive components, orthogonal tunability of f_0 and Q , notch frequency, notch depth, and THD. The comparison with previous designs, as given in Table 1, revealed that the proposed structure is very attractive because it requires fewer active and passive components. The proposed filter structure occupies less chip area as it does not require any resistors for its design. Also, it increases chip density, which is the requirement of the current scenario. The deeper the notch, the better the filter attenuates the frequencies within

the notch. However, it's worth noting that a filter with too deep of a notch may introduce other problems, such as phase distortion or group delay. Hence the design of a filter is a balancing act between achieving the desired notch depth and maintaining other essential performance characteristics.

The proposed structure offers a -52.9 dB notch depth, which is quite sufficient to eliminate the unwanted frequency. In the context of the dynamic range of the filters, THD is a vital parameter to consider because filters can introduce distortion to a signal, particularly in the presence of harmonics. In general, the lower the THD, the better the filter's performance. The proposed structure achieved a sufficiently low distortion of -55 dB.

6. CONCLUSIONS

A power line notch filter for wearable biomedical devices in wireless body area network applications has been implemented using a versatile current-mode block, the VDGA. The filter proposed in this study has demonstrated a moderate notching depth of -52.9 dB at 50 Hz, presenting a balanced compromise between notching and distortion. As indicated by the simulated results, the unwanted frequency was successfully rejected using the proposed filter. The recovered biosignal, free of 50Hz interference, was achieved, with other frequency components being conspicuously apparent at the output. The proposed filter yielded a total harmonic distortion (THD) of -55 dB. These findings suggest that the proposed filter possesses the necessary characteristics to render it suitable for biomedical detection systems. Future research may extend the proposed work to remove the fundamental frequency and its major harmonics.

REFERENCES

- [1] Park, S., Jayaraman, S. (2003). Enhancing the quality of life through wearable technology. IEEE Engineering in Medicine and Biology Magazine, 22(3): 41-48. <https://doi.org/10.1109/MEMB.2003.1213625>
- [2] Singh, S., Prasad, D. (2022). Wireless body area network (WBAN): A review of schemes and protocols. Materials Today: Proceedings, 49(8): 3488-3496.

- <https://doi.org/10.1016/j.matpr.2021.05.564>
- [3] Taji, B. (2019). Signal quality assessment in wearable ECG devices. PhD thesis School of Electrical Engineering and Computer Science, University of Ottawa.
- [4] Kalogiros, S., Noulis, T. (2016). Noise analysis and optimization of CMOS CCII+ based ECG systems. International Conference on Telecommunications and Signal Processing (TSP), Vienna, Austria, pp. 257-260. <https://doi.org/10.1109/TSP.2016.7760873>
- [5] Tobón, D.P., Falk, T.H., Maier, M. (2016). MS-QI: A modulation spectrum-based ECG quality index for telehealth applications. IEEE Transactions on Biomedical Engineering, 63(8): 1613-1622. <https://doi.org/10.1109/TBME.2014.2355135>
- [6] Orphanidou, C., Bonnici, T., Charlton, P., Clifton, D., Vallance, D., Tarassenko, L. (2015). Signal-quality indices for the electrocardiogram and photoplethysmogram: Derivation and applications to wireless monitoring. IEEE Journal of Biomedical and Health Informatics, 19(3): 832-838. <https://doi.org/10.1109/JBHI.2014.2338351>
- [7] Castro, D., Flix, P., Presedo, J. (2015). A method for context-based adaptive QRS clustering in real time. IEEE Journal of Biomedical and Health Informatics, 19(5):1660-1671. <https://doi.org/10.1109/JBHI.2014.2361659>
- [8] Satija, U., Ramkumar, B., Manikandan, M.S. (2018). Automated ECG noise detection and classification system for unsupervised healthcare monitoring. IEEE Journal of Biomedical and Health Informatics, 22(3): 722-732. <https://doi.org/10.1109/JBHI.2017.2686436>
- [9] Li, H.X., Zhang, J.Y., Wang, L. (2011). A fully integrated continuous-time 50-Hz notch filter with center frequency tunability. Annual International Conference of the IEEE Engineering in Medicine and Biology Society, Boston, MA, USA, pp. 3558-3562. <https://doi.org/10.1109/IEMBS.2011.6090593>
- [10] Khateb, F., Prommee, P., Kulej, T. (2022). MIOTA-based filters for noise and motion artifact reductions in biosignal acquisition. IEEE Access, 10: 14325-14338. <https://doi.org/10.1109/ACCESS.2022.3147665>
- [11] Ziarani, A.K., Konrad, A. (2002). A nonlinear adaptive method of elimination of power line interference in ECG signals. IEEE Transactions on Biomedical Engineering, 49(6): 540-547. <https://doi.org/10.1109/TBME.2002.1001968>
- [12] Zeinali Zadeh, M.M., Niketeghad, S., Amirfattahi, R. (2012). A PLL based adaptive power line interference filtering from ECG signals. The 16th CSI International Symposium on Artificial Intelligence and Signal Processing, Shiraz, Fars, pp. 490-496. <https://doi.org/10.1109/AISP.2012.6313797>
- [13] Tomasini, M., Benatti, S., Milosevic, B., Farella, E., Benini, L. (2016). Power line interference removal for high-quality continuous biosignal monitoring with low-power wearable devices. IEEE Sensors Journal, 16(10): 3887-3895. <https://doi.org/10.1109/JSEN.2016.2536363>
- [14] Neycheva, T.D., Dobrev, D.P. (2022). Design of fractional filters for power-line interference suppression in ECG signals. In 2022 XXXI International Scientific Conference Electronics (ET), Sozopol, Bulgaria, pp. 1-6. <https://doi.org/10.1109/ET55967.2022.9920330>
- [15] Ranjan, R.K., Choubey, C.K., Nagar, B.C., Paul, S.K. (2016). Comb filter for elimination of unwanted power line interference in biomedical signal. Journal of Circuits, Systems and Computers, 25(6): 1650052. <https://doi.org/10.1142/S0218126616500523>
- [16] Paul, S.K., Choubey, C.K., Tiwari, G. (2018). Low power analog comb filter for biomedical applications. Analog Integrated Circuits and Signal Processing, 97: 371-386. <https://doi.org/10.1007/s10470-018-1329-8>
- [17] Choubey, C.K., Sahani, A., Paul, S.K. (2016). Ultra-low power comb filter. 2016 IEEE International Conference on Advances in Electronics, Communication and Computer Technology (ICAECCT), Pune, India, pp. 164-166. <https://doi.org/10.1109/ICAECCT.2016.7942575>
- [18] Choubey, C.K., Paul, S.K. (2022). Nth order voltage-mode universal filter employing only plus type differential difference current conveyor. Analog Integrated Circuits and Signal Processing, 110: 197-210. <https://doi.org/10.1007/s10470-021-01967-z>
- [19] Tangsrirat, W., Channumsin, O. (2011). Voltage-mode multifunctional biquadratic filter using single DVCC and minimum number of passive elements. Indian Journal of Pure and Applied Physics, 49(10): 703-707.
- [20] Casper, B.K., Comer, D.J., Comer, D.T. (1999). An integrable 60-Hz notch filter. IEEE Transactions on Circuits and Systems II: Analog and Digital Signal Processing, 46(1): 74-77. <https://doi.org/10.1109/82.749101>
- [21] Feeri, G., Stornelli, V., Simone, A.D. (2011). A CCII-based high impedance input stage for biomedical applications. Journal of Circuits, Systems and Computers, 20(8): 1441-1447. <https://doi.org/10.1142/S021812661100802X>
- [22] Kumngern, M., Somdunyanok, M., Prommee, P. (2008). High-Input impedance voltage-mode multifunction filter with three-input single-output based on simple CMOS OTAs. International Symposium on Communications and Information Technologies, Vientiane, Laos, pp. 426-431. <https://doi.org/10.1109/ISCIT.2008.4700228>
- [23] Alzaher, H.A., Tasadduq, N., Mahnashi, Y. (2013). A highly linear fully integrated powerline filter for biopotential acquisition systems. IEEE Transactions on Biomedical Circuits and Systems, 7(5): 703-712. <https://doi.org/10.1109/TBCAS.2013.2245506>
- [24] Aqueel, A., Ansari, M.S., Maheshwari, S. (2017). Subthreshold CMOS low-transconductance OTA based low-pass notch for EEG applications. International Conference on Multimedia, Signal Processing and Communication Technologies (IMPACT), Aligarh, India, pp. 247-251. <https://doi.org/10.1109/MSPCT.2017.8364014>
- [25] Zhang, J., Chan, S.C., Li, H., Zhang, N., Wang, L., (2020). An area-efficient and highly linear reconfigurable continuous-time filter for biomedical sensor applications. Sensors, 20(7): 2065. <https://doi.org/10.3390/s20072065>
- [26] Jaikla, W., Siripongdee, S., Khateb, F., Sotner, R., Silapan, P., Suwanjan, P., Chaichana, A. (2021). Synthesis of biquad filters using two VD-DIBAs with independent control of quality factor and natural frequency. AEU-International Journal of Electronics and Communications, 132: 153601. <https://doi.org/10.1016/j.aeue.2020.153601>
- [27] Hirunporm, J., Siripruchyanun, M. (2020). An

- independently/electronically controllable schmitt trigger using only single VDGA. International Conference on Electrical Engineering/Electronics, Computer, Telecommunications and Information Technology (ECTI-CON), Phuket, Thailand, pp. 118-121. <https://doi.org/10.1109/ECTI-CON49241.2020.9158058>
- [28] Satansup, J., Tangsrirat, W. (2015). Single VDGA-based first-order all pass filter with electronically controllable passband gain. 7th International Conference on Information Technology and Electrical Engineering (ICITEE), Chiang Mai, Thailand, pp. 106-109. <https://doi.org/10.1109/ICITEED.2015.7408922>
- [29] Channumsin, O., Tangsrirat, W. (2020). Compact dual-mode SITO universal filter and quadrature oscillator with only single VDGA. 17th International Conference on Electrical Engineering/Electronics, Computer, Telecommunications and Information Technology (ECTI-CON), Phuket, Thailand, pp. 181-184. <https://doi.org/10.1109/ECTI-CON49241.2020.9158232>
- [30] Satansup, J., Tangsrirat, W. (2013). CMOS realization of voltage differencing gain amplifier (VDGA) and its application to biquad filter. *Industrial Journal Engineers Materials Science*, 20(6): 457-464.
- [31] Choubey, C.K., Paul, S.K. (2020). Implementation of chaotic oscillator by designing a simple Chua's diode using a single VDTA. *AEU - International Journal of Electronics and Communications*, 124: 153360, <https://doi.org/10.1016/j.aeue.2020.153360>
- [32] Choubey, C.K., Paul, S.K. (2022). Systematic realisation of inductorless and resistorless Chua's chaotic oscillator using VDGA. *International Journal of Electronics*, 110(1): 1006-1027. <https://doi.org/10.1080/00207217.2022.2068200>
- [33] Moody, G.B., Mark, R.G. (2001). The impact of the MIT-BIH arrhythmia database. *IEEE Engineering in Medicine and Biology Magazine*, 20(3): 45-50. <https://doi.org/10.1109/51.932724>